Aquatic ecological modelling with TELEMAC3D: performance of the ecological library AED2 in a natural ecosystem

Francesco Piccioni, Brigitte Vinçon-Leite, Minh-Hoang Le, Céline Casenave

Aquatic ecological modelling with TELEMAC3D: performance of the ecological library AED2 in a natural ecosystem

Francesco Piccioni, Brigitte Vinçon-Leite
LEESU, Ecole des Ponts ParisTech, UPEC
Champs-sur-Marne, France
francesco.piccioni@enpc.fr

Minh-Hoang Le
LHSV, Ecole des Ponts ParisTech, CEREMA, EDF R&D
Chatou, France

Céline Casenave
UMR MISTEA, Univ Montpellier, INRA, Montpellier SupAgro, Montpellier, France

***Abstract*—This work aims to test the performance of the coupled models TELEMAC-3D / AED2 for reproducing over a seasonal time-horizon the complete phytoplankton growth-cycle. The study site is a small and shallow urban lake that suffers from repeated and severe harmful algal blooms, located in the east of the Great Paris metropolitan area. The lake is equipped with sensors recording data at high-frequency (every 10 minutes) of water temperature, pH, as well as concentrations of dissolved oxygen, nitrate total chlorophyll and phycocyanin. Such an extensive data set allows to test the model thoroughly against multiple variables and at different time scales. In particular, simulation results were evaluated in terms water temperature at different depths to test the ability of the coupled models to simulate thermal stratification in a shallow water body. High-frequency observations of total chlorophyll, phycocyanin, nitrate, dissolved oxygen concentrations, were used to calibrate the biogeochemical model and evaluate its performance. The analysis of model results highlights a feedback between the coupled models, that can be linked to the dynamic calculation of the light extinction coefficient done in the biogeochemical model. The coupled models AED2 and TELEMAC-3D allow to correctly reproduce the overall seasonal phytoplankton growth in a water body, correctly dispatching biomass among the different phytoplankton groups in particular during summer. Furthermore, the model reproduces correctly the overall dynamics recorded in the study site in terms of dissolved oxygen and nitrate. This corroborates the robustness of the coupled models and of the configuration set up for this study.**

I. INTRODUCTION

Water resources are highly impacted by anthropogenic stressors. Urbanization can lead to an increase of pollutant and nutrient input to aquatic ecosystems, enhancing eutrophication [1]. Furthermore, their thermal dynamics are also affected by climate change. Warmer water temperatures and accelerated eutrophication are thought to be the main causes of the expansion of harmful algal blooms observed worldwide during the last decades [2]–[4]. In particular, because of their potential toxicity, cyanobacteria blooms are an ever increasing concern in the management of water resources and represent a serious threat for the balance of aquatic ecosystems [3], [5]. For these reasons, an ever-increasing interest grows around modelling tools capable of simulating the ecological evolution of aquatic ecosystems under different meteorological or eutrophication scenarios, in order to provide stakeholders with reliable projections for decision making [6]. In this context, TELEMAC-3D has recently been coupled by EDF R&D with the well-known ecological library Aquatic EcoDynamics (AED2). Aquatic ecological models often have a complex structure with a high number of parameters to be defined and their calibration is challenging: data deriving from traditional periodic field surveys are sparse in space and time and do not allow for a thorough validation of processes occurring at a time-scale lower than the monitoring frequency.

The aim of our work is to test the performance of the coupled model TELEMAC-3D / AED2 on a full scale experimental site over a seasonal time-horizon with the objective of reproducing the phytoplankton succession. The study site is a small and shallow urban lake located in the east of Great Paris metropolitan area, which suffers from repeated and severe harmful algal blooms during spring, summer and autumn. Aside from the traditional monitoring via field campaigns and water sampling, the study site is equipped with specific sensors recording data at high-frequency (every 10 minutes) of water temperature as well as concentrations of dissolved oxygen, nitrate, total chlorophyll and phycocyanin, which is considered a proxy for cyanobacteria biomass. Such an extensive data set allows to test the model thoroughly against multiple variables and at different time scales.

II. MATERIALS AND METHODS

A. *Study site and measuring instrumentation*

The study site is Lake Champs-sur-Marne. It is a sand-pit lake located in the East of Paris (latitude: 48°51'50" N, longitude: 2°35'52" E), next to the Marne River. It is a small and shallow water body with a surface of 0.12 km^2, mean depth of 2.5 m and maximum depth of around 3.5 m. As shown in Fig. 1, the lake is deeper in the southern part, while depth decreases to under 2 m in the northern part of the lake.

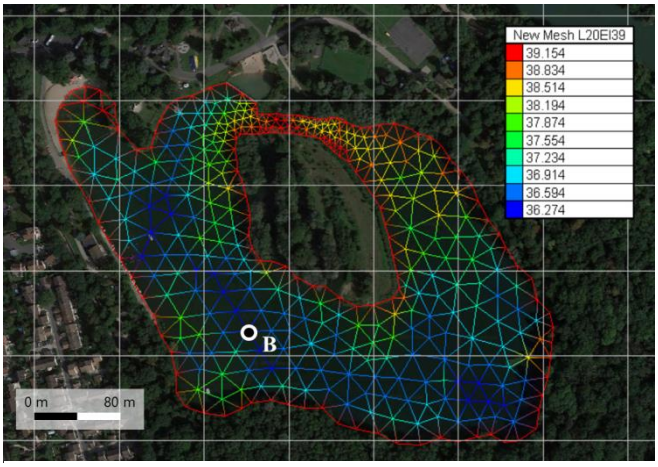

Figure 1: Satellite picture of Lake Champs-sur-Marne and computational domain used for the present study. The colour chart shows the elevation of each point of the grid in meters above sea level and the white dot indicates the measuring site.

The lake is fed primarily by groundwater, and has no inflows nor outflows. Its water level is influenced by the Marne River that flows from east to west right north of the lake. The lake level varies weakly during the year, with monthly oscillations lower than 0.2 m on average.

Given its shallowness, Lake Champs-sur-Marne is polymyctic and its thermal behaviour is strongly influenced by the meteorological conditions. Between Spring and Autumn, periods of stable thermal stratification that can last up to two or three continuous weeks alternate with complete mixing and overturn of the water column. The lake suffers from strong eutrophic conditions and experiences severe harmful algal blooms, especially between early spring and autumn. These blooms are often dominated by potentially toxic species of cyanobacteria.

For these reasons, the lake is monitored through periodical field surveys during which water samples, profiles and Secchi depth measurements are collected, as well as continuous *in situ* measurements that record data at high-frequency (every 10 min) of relevant physical, biological and chemical variables. In particular, measuring site B (see figure 1) is equipped with two SP2T10 (nke INSTRUMENT®) water temperature sensors at the surface (0.5 m depth) and bottom (2.5 m depth) layers, while at the middle of the water column (1.5 m depth), the MPx multi-parameter sensor (nke INSTRUMENT®) records data in terms of water temperature and total chlorophyll, dissolved oxygen and phycocyanin concentrations. A detailed description of the automated measuring system can be found in [7]. Eventually, high-frequency observations of nitrate concentration are also recorded at 1.5 m depth at site B, through the OPUS UV spectral sensor (OPUS instrumentation). Such data are used in this work to calibrate the model parameters and evaluate the its performance.

B. *Model configuration*

TELEMAC3D (release 8.1.2) coupled with the ecological library Aquatic EcoDynamics is used to run 3D simulations of the thermal dynamics and of the biogeochemical cycle in Lake Champs-sur-Marne. The simulated period covers the season of phytoplankton growth observed on the study site during the year 2019 and goes from the month of February to the end of October.

In the coupled model, TELEMAC3D handles the hydrodynamics, while AED2, through a set of partial differential equations, simulates the biogeochemical cycle [8]. Namely, the AED2 library is called at each time step in order to update the concentration of the variables simulated in the biogeochemical cycle, which are then treated as active tracers by TELEMAC3D. When TELEMAC3D is coupled with AED2, the light extinction coefficient is dynamically calculated at each iteration by AED2 as a function of tracers concentrations and the corresponding specific light extinction coefficients that can be set by the user [8]. This way, AED2 can have a feedback on the TELAMAC3D results in particular in terms of vertical distribution of water temperature and thermal stratification.

The computational domain used to run the coupled models is shown in Fig. 1. It was built with the open-source software BlueKenue™ [9]. It consists of a triangular grid with an average distance between the nodes of 20 m, and a refined zone around the narrower portion of the water body. Bathymetric data were obtained via an echo-sounder. The mesh is composed of 404 nodes (661 elements), with 10 σ-layers for the discretization on the vertical axis and a uniform water level set at an elevation of 40 m a.s.l..

Hydrodynamic model

The Nezu and Nakagawa's formulation of the mixing length model with Viollet's damping function was implemented for vertical turbulence closure. The molecular diffusivity of water is used on the vertical as a background value and was set to 10^{-6} m^2s^{-1}, while horizontal diffusivity was set to 0.01 m^2s^{-1} after similar applications ([10], [11]) and according to the grid size [12]. The model is forced with six meteorological variables: relative humidity [-], air temperature [°C], cloud cover [-], net solar radiation [$J\ s^{-1}m^{-2}$], wind speed [$m\ s^{-1}$] and direction [°N]. Their values were downloaded from the closest Meteo France meteorological station, located at the Orly airport roughly 40 km south-west of the study site. In the heat budget, the contribution of precipitation was neglected both in terms of energy and mass, while for evaporation only the mass flux was neglected. Finally, the model was run with a 60 s time step, and its outputs were saved with a four-hours time step.

Biogeochemical model

Aquatic EcoDynamics (AED2) was recently coupled with the TELEMAC system. AED2 is a modular biogeochemical library, that potentially allows the user to simulate all the processes playing a role in the biogeochemical cycle in aquatic ecosystems, from benthic fluxes and microbial decomposition to primary production,

grazing, and macrophytes growth [8]. The model configuration can be customized by the user through the activation and deactivation of its modules. For the present work, focused on phytoplankton growth, five modules were activated, which are listed in Table 1 together with the relative variables simulated by AED2 and their initial conditions. In the table, particulate (dissolved) fractions of organic carbon, nitrogen and phosphorus are respectively indicated as POC, PON and POP (DOC, DON and DOP). Four phytoplankton groups typically observed on the study site are activated in this configuration: cyanobacteria, green algae, flagellates and diatoms.

Table 1: Modules and variables activated in AED2, along with their initial conditions.

Module	Simulated variables	Initial value
Oxygen	Dissolved oxygen	180 mmol O m^{-3}
Phosphorus	Ortho-phosphate	2.6 mmol P m^{-3}
Nitrogen	Ammonium	40 mmol N m^{-3}
	Nitrate	45 mmol N m^{-3}
Organic matter	POC	310 mmol C m^{-3}
	PON	37 mmol N m^{-3}
	POP	1.5 mmol P m^{-3}
	DOC	600 mmol C m^{-3}
	DON	37 mmol N m^{-3}
	DOP	1.5 mmol P m^{-3}
Phytoplankton	Cyanobacteria	1 mmol C m^{-3}
	Green algae	1 mmol C m^{-3}
	Flagellates	1 mmol C m^{-3}
	Diatoms	6 mmol C m^{-3}

C. Initialization and calibration of the model

Data measured at site B were used to initialize the model, uniformly over the study site. High frequency observations allowed to directly set the initial conditions in terms of water temperature, total phytoplankton concentration, dissolved oxygen concentration and nitrate concentration. Water samples collected during two field campaigns carried out in January and February of 2019 granted data to initialize the remaining variables listed in Table 1. Eventually, no data were available to set the initial velocity field, and the model was therefore initialized with water at rest.

The coupled models were calibrated against high-frequency observations recorded at site B in terms of water temperature (at three different layers) and total chlorophyll, cyanobacteria and dissolved oxygen concentration at the middle layer. The calibration of the coupled models was done by trial and error and involved three parameters from the TELEMAC3D hydrodynamic model, deputed to tune the heat-transfer model at the air-water interface, and around 40 parameters proper of the AED2 library. Such parameters were selected as the most sensitive from previous sensitivity analysis. The AED2 parameters were initially set and calibrated based on values found in similar applications in scientific literature (e.g. [8], [13], [14]). The main parameters included in the calibration of the coupled TELEMAC3D and AED2 models are listed in table 2.

In this study, the coupled models were calibrated focusing on the months from February to July of 2019, while they were run for validation until the end of October. In order to evaluate the model performances, the root mean square error (RMSE) between model results and observations was calculated. High-frequency observations were therefore averaged in order to match the model output time step.

Table 2: Calibrated values of the most relevant parameters included in the present TELEMAC3D / AED2 configuration.

Model	Parameter	Value	Unit			
T3D	Coeff. for atm. rad.	0.89	-			
	Coeff. for surf. Water rad.	0.93	-			
	Coeff. for atm.-wat. heat exc.	0.0017	-			
AED	Light ext. coeff. (DOM)	0.002	m^2 $mmol$ C^{-1}			
	Light ext. coeff. (POM)	0.002	m^2 $mmol$ C^{-1}			
	Phytoplankton					
		Green	**Cyano.**	**Falg.**	**Diat.**	**Unit**
	Growth rate (20°C)	1.4	1.2	1.6	3.7	d^{-1}
	Temp. coeff. for growth	1.08	1.08	1.08	1.05	-
	Std. wat. temp.	20	20	18	4	°C
	Opt. wat. temp.	25	28	23	9	°C
	Max. wat. temp.	35	36	30	18	°C
	Light ext. coeff.	0.005	0.005	0.01	0.005	m^2 $mmol$ C^{-1}
	Half sat. const. for light	28	25	28	10	μE m^{-2} s^{-1}

III. RESULTS

Model results at site B in terms of water temperature and concentration of total chlorophyll, cyanobacteria, dissolved oxygen and nitrate are gathered in figures 2 and 3, together with the corresponding observations from high-frequency measurements. The performance of the coupled models is here analysed over the whole simulation period in two separate sections: one concerning the thermal and stratification dynamics, and the second one dealing with the biogeochemical cycle.

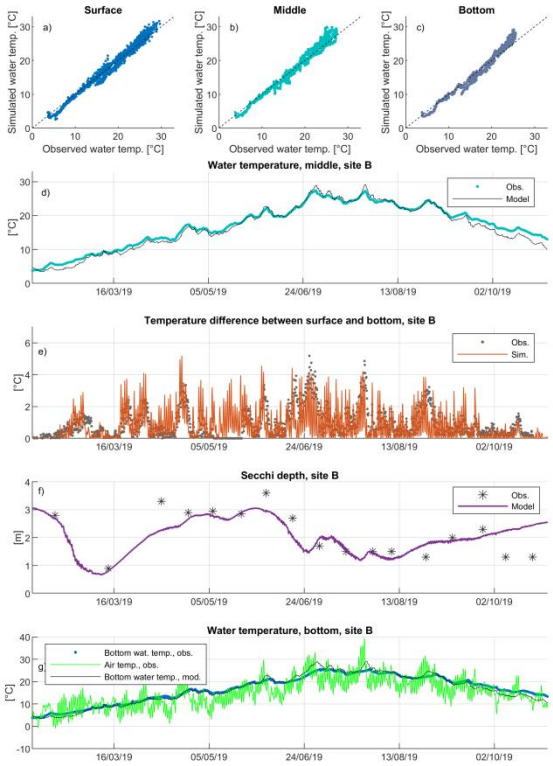

Figure 2: Model results for the seasonal simulation in 2019 in terms of water temperature and Secchi depth. Panels a, b and c: parity diagrams for water temperature at the surface, middle and bottom layers respectively. Panel d: observations and simulation results in terms of water temperature for the middle layer. Panel e: observed and simulated water temperature difference between the surface and bottom layers. Eventually, panel f shows the simulated and observed values for Secchi depth, and panel g shows the comparison between observed and simulated bottom water temperature and the air temperature series used to force the model. All figures are referred to measuring site B.

D. Thermal dynamics

Model results in terms of water temperature are compared with high-frequency observations at site B in figure 2. The parity diagrams in panels a, b and c show a very good agreement between simulated and observed water temperature for all the three layers, with only a small overestimation by the model of the highest temperatures recorded on the study site (in particular for the surface layer) and a slight underestimation of lower water temperatures. Figure 2d shows, as an example for the middle layer, that the evolution of water temperature over the simulation period is correctly reproduced by the coupled models. This is confirmed by the low RMSE values between simulated and observed water temperature at all three layers: respectively of 1.09°C, 1.16°C and 1.20°C for the surface, middle and bottom layers relatively to the whole simulation period.

Figure 2d shows particularly good model performances in terms of water temperature until the end of the month of September. Afterwards, however, a deterioration of the model performance is detectable with an underestimation of water temperature by the model. Similar results were obtained for the surface and bottom layers. Such behaviour was further analysed by comparing the simulated water temperature at site B with the air temperature values used to force the model. Such comparison (Figure 2f) showed how, between the months of October and November, simulated water temperature follows closely the data of air temperature used to force the model. This might be linked with some of the processes neglected in the present configuration, such as water level variations or interactions with groundwater, that might influence the real system.

Between spring and autumn, numerous thermal stratification events are observed on the study site. Such stratification events can last up to two or three consecutive weeks and might reach water temperature differences between the surface and bottom layers around 6°C [11], as shown by panel e of Figure 2. The analyses of the differences between surface and bottom water temperature showed that the model correctly reproduced the stratification events observed on the study site, in particular during the spring season. However, during the months of June and July, when the highest water temperatures are reached, the simulated bottom water temperature is slightly overestimated by the model, causing simulated stratification to be somewhat weaker than the observed one. This could be caused by an underestimation of the light extinction dynamically computed by AED2. To test this hypothesis, the simulated light extinction coefficient (K_d) was calculated over the whole simulation period following equation [8]:

$$K_d = K_w + K_{e,DOC}DOC + K_{e,POC}POC + \sum_{i}^{N_{PHY}} K_{e,i}PHY_{C,i}$$

where K_w is the base light extinction coefficient associated with water, and $K_{e,DOC}$, $K_{e,POC}$ and K_{e_i} represent respectively the specific light extinction coefficient for dissolved organic carbon, particulate organic carbon and for the phytoplankton group i, whose values were known parameters of the model. The concentration of POC, DOC and phytoplankton (PHY_{Ci}) were known as output of the model simulation. Eventually, the light extinction coefficient could be converted into its corresponding simulated Secchi depth S through the Poole and Atkins equation ($S=1.7/K_d$, [15]).

The simulated and measured Secchi depth at site B are shown in figure 2f. The simulated values match closely with the observations, with only four main exceptions (namely in the months of April, June and October). Ultimately, therefore, the slight underestimation of summer thermal stratification found in model results could be partly linked with some simplifications made in the model configuration, such as the constant water level or the absence of exchanges with groundwater. Furthermore, an excess of numerical diffusion might also be introduced by the computational schemes of the hydrodynamic model and could have an impact on model results in terms of thermal stratification, especially on such a shallow water body.

E. Biogeochemical model

The calibration of the model was done by trial and error, comparing its results with high-frequency observations of total chlorophyll, cyanobacteria, dissolved oxygen and nitrate concentration. The analysis of such observations data set,

represented through the dotted grey lines in figure 3, shows the presence of a first strong peak of phytoplankton biomass around the beginning of March that surpasses 100 µg l^{-1} of total chlorophyll concentration. It constitutes the strongest bloom of the simulated period and completely consumes the stock of nitrate present in the water column, influencing the subsequent availability of nutrients (and nitrate in particular) to sustain phytoplankton growth during the remaining growing season.

Model results are also shown in figure 3 (coloured solid lines), in terms of total chlorophyll (panel a), cyanobacteria (panel b), dissolved oxygen (panel c) and nitrate concentration (panel d). In terms of total chlorophyll (Fig. 2a), the model reproduces correctly the overall behaviour recorded by the high-frequency sensor. The first algal bloom is correctly simulated, both in terms of timing and intensity. Following, the model correctly reproduces the decrease of phytoplankton biomass, as well as the span and overall concentration magnitude of the phytoplankton during the summer months. Eventually, the end of the growing season is also well captured by the model around the end of October.

The year 2019 was not characterized by particularly strong cyanobacterial blooms. As shown by Fig. 3b, their maximal concentration reaches roughly 40 µg Chl l^{-1} in four separate occasions: once during the late winter bloom, and the remaining times during sudden growth peaks between the end of August and the beginning of October. However, in the present configuration, the group representing cyanobacteria is adapted to warm water temperatures (i.e. optimum temperature of 28°C), and is therefore not capable to reproduce their winter growth. In this configuration in fact, winter growth completely deputed to the diatoms group, which are here parameterized with the lowest optimum temperature (i.e. 9°C). Similarly to what was discussed for total chlorophyll, during Summer the model manages to correctly simulate the span of the growing season for the group of cyanobacteria, as well as their overall concentration magnitude. However, the model fails to reproduce the succession of short term peaks detected by the high-frequency observations.

The dynamics of dissolved oxygen simulated by the model fits very closely that recorded by the high-frequency measurements. Figure 3c shows that the model overestimates slightly the concentration of dissolved oxygen, in particular during the colder months of the simulation: during the strong late winter phytoplankton bloom, as well as during the month of October. In the remaining months of simulation dissolved oxygen concentration is correctly reproduced.

Figure 3d shows the comparison between high-frequency observations and model results at site B in terms of nitrate concentration. The model correctly reproduces the observed nitrate dynamics before and during the late-winter algal bloom. The initial increase in nitrate concentration is modelled here solely through the processes of mineralization of organic matter and nitrification of ammonium. The rapid consumption of all the available nitrate during the late winter algal bloom is also correctly simulated.

Right after the late-winter bloom, during the months of April and May, the phytoplankton observations are very low and correspond to an increase in the observed nitrate concentrations. The nitrate accumulated in the water column during this period is then quickly consumed at the beginning of the second blooming period around the month of June. The lake appears to be nitrogen limited from this point until the end of the growing season. These dynamics are not fully reproduced by the model. At the end of the late-winter bloom the simulated phytoplankton concentration is higher than the observed one, causing, in the model, a stronger consumption of nitrate by the phytoplankton, and ultimately delaying the simulated accumulation of nitrate. Such accumulation of nitrate is necessary to the model in order to sustain phytoplankton growth during the subsequent summer and autumn months. Eventually, at the end of the growing season, in the last portion of the simulation around the end of October, a strong increase of nitrate concentration is recorded in the study site. The model also simulates an increase of nitrate concentration during the month of October, but with a considerably lower rate. In the present model configuration, no external input of nutrients are present, and such nitrate increase is obtained solely through the processes of organic matter mineralization and nitrification. The underestimation of nitrate increase by the model suggests the existence of nitrogen sources into the ecosystem that are not taken into account in the present configuration.

IV. DISCUSSION

In this work, the coupled models TELEMAC3D and AED2 were implemented on Lake Champs-sur-Marne, and were used to simulate the biogeochemical cycle in the study site during the complete phytoplankton growth season recorded in the year 2019, i.e. from February to October.

In their own fields of application, the two models are both well-established tools that, separately, have been employed in various contexts (e.g., for TELEMAC3D: [16]–[18], and [14], [19], [20] for AED2). The coupling of the two models introduces the possibility of modelling the biogeochemical cycle directly through the TELEMAC modelling system. In this work, it was possible to test the behaviour of the coupled models in a natural lake ecosystem and the use of high-frequency observations allowed to evaluate the performance of the models continuously over the simulation period.

During the seasonal simulation of 2019, the coupled models reproduced well the overall water temperature dynamics at all three layers. The underestimation of water temperature found at the end of the simulation for the month of October, as well as the slight overestimation of summer water temperature, could be linked with some of the simplifications introduced in the present configuration, such as a constant water level and the absence of exchanges with groundwater. The latter in particular could somewhat moderate the seasonal variations of water temperature in the real system. Despite some differences with the measured water temperature series, the overall RMSE values between model and observations were lower than 1.2°C. Similar

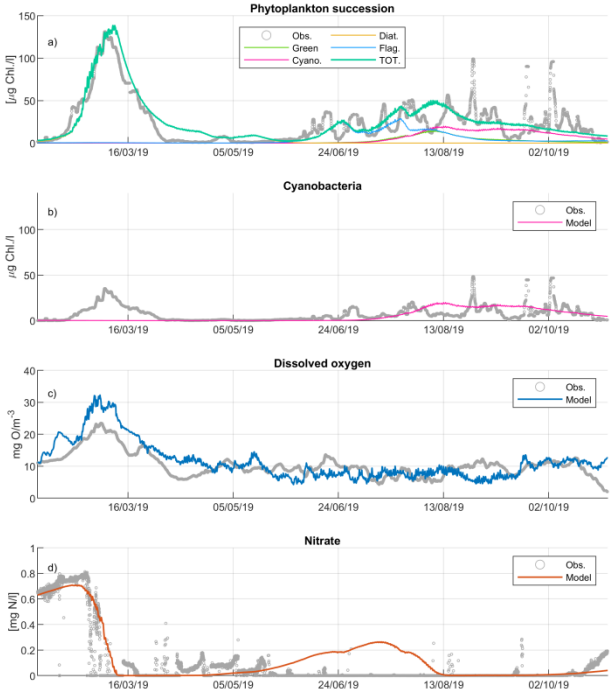

Figure 3: Model results and high-frequency observations in terms of: total chlorophyll (panel a), cyanobacteria concentration (panel b), dissolved oxygen concentration (panel c), and nitrate concentration (panel d). Coloured lines represent model results and grey dotted lines the observation series; all figures are referred to site B.

values are usually considered as good model performances in scientific literature (e.g. [11], [21], [22]). Furthermore, starting in particular from the month of October until the end of January, very low phytoplankton biomass is usually detected on the study site. In this respect, the bias found for water temperature during early autumn should have a reduced impact on the outcomes of the coupled biogeochemical model. Water temperature is a key variable for the simulation of the biogeochemical cycle and in particular for phytoplankton growth. Despite some slight biases, water temperature was overall very well simulated by the coupled models over the simulated period.

This study is focused on phytoplankton growth and on cyanobacteria growth in particular, and the modules activated in the configuration of AED2 (see Table 1) reflect this general objective. Furthermore, the availability of an extensive high-frequency data set allowed to test the model thoroughly, against multiple variables that characterize the biogeochemical cycle exhaustively: in terms of total phytoplankton, cyanobacteria and dissolved oxygen concentration, as well as in terms of an important nutrient such as nitrate.

The biogeochemical cycle was correctly reproduced over the eight months of the simulation. Total phytoplankton concentration was analysed here through phytoplankton chlorophyll content. The four algal groups activated in the present configuration (diatoms, flagellates, green algae and cyanobacteria) are typically related to different optimum water temperatures. Among them, diatoms are usually linked with the lowest optimum water temperatures, while cyanobacteria are typically linked with the highest ones [3]. Following this general assumption, they were here parameterized to respond different optimum water temperatures. This choice allowed the model to correctly reproduce the overall magnitude of total chlorophyll concentration over the simulated period.

The observed late winter phytoplankton bloom showed a considerable presence of cyanobacteria. However, due to the parameterization of their optimum water temperature, cyanobacteria growth is inhibited at low water temperatures. This shows the need to introduce various *genera* of the same algal group with different parameterizations, in order to mimic the complexity of a natural ecosystem.

Also the remaining variables recorded *in situ* (i.e. dissolved oxygen, nitrate, Secchi depth) were well reproduced by the model for 2019. However, some discrepancies were indeed detected when comparing model results to high-frequency observations. Notably, the model did not fully reproduce the sudden peaks of growth and mortlity observed during spring and summer. This could be explained by the absence, in the models configuration, of: (i) nitrogen-fixing cyanobacteria such as *Aphanizomenon*, present on the study site, that should be advantaged under nitrogen-limited conditions, (ii) predation by zooplankton or competition for nutrients and light with other organisms, such as macrophytes, and (iii) by the absence in the model configuration of external nutrient sources, that might locally boost phytoplankton growth over a short period of time.

Furthermore, the underestimation of nitrate accumulation during early autumn could be simply originated by an underestimation of the mineralization rate of organic matter implemented in the present configuration.

V. CONCLUSION

In this work, the recent coupling between TELEMAC3D and the biogeochemical library AED2 was tested in a natural ecosystem, Lake Champs-sur-Marne, for which an extensive data set is available. In particular, the availability of high-frequency *in situ* data of variables particularly relevant to the biogeochemical cycle, such as water temperature, dissolved oxygen total chlorophyll, cyanobacteria and nitrate concentrations, allowed to thoroughly test the performance of the coupled models all along the simulation period. In particular, the results show a correct simulation of the light extinction coefficient and highlight the feedback of its dynamic calculation, computed through AED2, on the hydrodynamic model. Furthermore, results show how the mineralization of organic matter can suffice to sustain phytoplankton growth over an annual cycle in the simulation of an ecosystem without direct surface inlets. Through the coupling with AED2, the TELEMAC system is capable of correctly simulating the main features of the biogeochemical cycle and, in particular, phytoplankton growth over a complete growth season.

ACKNOWLEDGEMENT

The authors acknowledge the Base de loisirs du lac de Champs/Marne (CD93) for their logistic support in the field

campaigns. The dataset used for model calibration and validation was collected under the OSSCyano (ANR-13-ECOT-0001) and ANSWER (ANR-16-CE32-0009-02) projects. The environmental observatories OSU EFLUVE and OLA contributed to the financial support for equipment maintenance. The first author's PhD grant is funded by Ecole des Ponts ParisTech and the ANSWER project.

REFERENCES

[1] D. M. Anderson, P. M. Glibert, and J. M. Burkholder, "Harmful algal blooms and eutrophication: Nutrient sources, composition, and consequences," *Estuaries*, vol. 25, no. 4, pp. 704–726, Aug. 2002, doi: 10.1007/BF02804901.

[2] J. Heisler *et al.*, "Eutrophication and Harmful Algal Blooms: A Scientific Consensus," *Harmful Algae*, vol. 8, no. 1, pp. 3–13, Dec. 2008, doi: 10.1016/j.hal.2008.08.006.

[3] H. Paerl and T. Otten, "Harmful Cyanobacterial Blooms: Causes, Consequences, and Controls," *Microbial ecology*, vol. 65, Jan. 2013, doi: 10.1007/s00248-012-0159-y.

[4] J. M. O'Neil, T. W. Davis, M. A. Burford, and C. J. Gobler, "The rise of harmful cyanobacteria blooms: The potential roles of eutrophication and climate change," *Harmful Algae*, vol. 14, pp. 313–334, Feb. 2012, doi: 10.1016/j.hal.2011.10.027.

[5] L. Bláha, P. Babica, and B. Maršálek, "Toxins produced in cyanobacterial water blooms – toxicity and risks," *Interdiscip Toxicol*, vol. 2, no. 2, pp. 36–41, Jun. 2009, doi: 10.2478/v10102-009-0006-2.

[6] D. Trolle *et al.*, "A community-based framework for aquatic ecosystem models," *Hydrobiologia*, vol. 683, no. 1, pp. 25–34, Mar. 2012, doi: 10.1007/s10750-011-0957-0.

[7] V. Tran Khac *et al.*, "An Automatic Monitoring System for High-Frequency Measuring and Real-Time Management of Cyanobacterial Blooms in Urban Water Bodies," *Processes*, vol. 6, no. 2, p. 11, Jan. 2018, doi: 10.3390/pr6020011.

[8] M. R. Hipsey, L. C. Bruce, and D. P. Hamilton, "Aquatic Ecodynamics (AED) Model Library. Science Manual.," Oct. 2013, [Online]. Available: http://aed.see.uwa.edu.au/research/models/aed/Download/AED_ScienceManual_v4_draft.pdf

[9] Canadian Hydraulic Centre, *Blue Kenue reference manual*. Ottawa, Ontario, Canada, 2011.

[10] F. Soulignac *et al.*, "Performance Assessment of a 3D Hydrodynamic Model Using High Temporal Resolution Measurements in a Shallow Urban Lake," *Environ Model Assess*, vol. 22, no. 4, pp. 309–322, Aug. 2017, doi: 10.1007/s10666-017-9548-4.

[11] F. Piccioni, C. Casenave, B. J. Lemaire, P. Le Moigne, P. Dubois, and B. Vinçon-Leite, "The thermal response of small and shallow lakes to climate change: new insights from 3D hindcast modelling," *Earth System Dynamics*, vol. 12, no. 2, pp. 439–456, Apr. 2021, doi: 10.5194/esd-12-439-2021.

[12] A. Okubo, "Oceanic diffusion diagrams," *Deep Sea Research and Oceanographic Abstracts*, vol. 18, no. 8, pp. 789–802, Aug. 1971, doi: 10.1016/0011-7471(71)90046-5.

[13] G. Gal, M. Hipsey, A. Parparov, U. Wagner, V. Makler, and T. Zohary, "Implementation of ecological modeling as an effective management and investigation tool: Lake Kinneret as a case study," *Ecological Modelling*, vol. 220, pp. 1697–1718, Jun. 2009, doi: 10.1016/j.ecolmodel.2009.04.010.

[14] A. Fenocchi, M. Rogora, G. Morabito, A. Marchetto, S. Sibilla, and C. Dresti, "Applicability of a one-dimensional coupled ecological-hydrodynamic numerical model to future projections in a very deep large lake (Lake Maggiore, Northern Italy/Southern Switzerland)," *Ecological Modelling*, vol. 392, pp. 38–51, Jan. 2019, doi: 10.1016/j.ecolmodel.2018.11.005.

[15] H. H. Poole and W. R. G. Atkins, "Photo-electric Measurements of Submarine Illumination throughout the Year," *Journal of the Marine Biological Association of the United Kingdom*, vol. 16, no. 1, pp. 297–324, May 1929, doi: 10.1017/S0025315400029829.

[16] C. Villaret, J.-M. Hervouet, R. Kopmann, U. Merkel, and A. G. Davies, "Morphodynamic modeling using the Telemac finite-element system," *Computers & Geosciences*, vol. 53, pp. 105–113, Apr. 2013, doi: 10.1016/j.cageo.2011.10.004.

[17] J. Feng and M. Jodeau, "Three-dimensional numerical modeling of sediment transport with TELEMAC-3D: validation of test cases," p. 9, 2016.

[18] U. H. Merkel, "Thermal Stratification in Small Lakes with TELEMAC-3D: Showcase 'Lake Monsterloch,'" *XXVIth TELEMAC-MASCARET User Conference, 15th to 17th October 2019, Toulouse*, 2019, doi: 10.5281/zenodo.3611576.

[19] L. Zhang, M. R. Hipsey, G. X. Zhang, B. Busch, and H. Y. Li, "Simulation of multiple water sources ecological replenishment for Chagan Lake based on coupled hydrodynamic and water quality models," *Water Science and Technology: Water Supply*, p. ws2017079, May 2017, doi: 10.2166/ws.2017.079.

[20] A. I. Krinos, K. J. Farrell, V. Daneshmand, K. C. Subratie, R. J. Figueiredo, and C. C. Carey, "Including variability in air temperature warming scenarios in a lake simulation model highlights uncertainty in predictions of cyanobacteria," *bioRxiv*, p. 734285, Aug. 2019, doi: 10.1101/734285.

[21] M. R. Magee and C. H. Wu, "Response of water temperatures and stratification to changing climate in three lakes with different morphometry," *Hydrology and Earth System Sciences*, vol. 21, no. 12, pp. 6253–6274, 2017, doi: 10.5194/hess-21-6253-2017.

[22] S. Moras, A. I. Ayala, and D. C. Pierson, "Historical modelling of changes in Lake Erken thermal conditions," *Hydrology and Earth System Sciences*, vol. 23, no. 12, pp. 5001–5016, Dec. 2019, doi: https://doi.org/10.5194/hess-23-5001-2019.